

<https://doi.org/10.70731/b3b1q080>

Spatiotemporal Characteristics of Built Environment Impacts on Street Vitality in Central Nanchang: A Multiscale Geographically Weighted Regression Approach

Zheng Gong ^a, Qiyang Zhao ^{a,*}, Wentao Song ^a, Zhiling Jian ^a

^a School of Earth Sciences, East China University of Technology, Nanchang 330013, China

KEYWORDS

Street Vitality;
Built Environment;
Multiscale Geographically
Weighted Regression
(MGWR);
Street View Imagery;
Nanchang City

ABSTRACT

Exploring the impact of the built environment on street vitality is essential for enhancing urban public spaces. Using the central urban area of Nanchang City as a case study, multi-temporal street vitality is measured with population heat data. A multi-dimensional built environment indicator system is developed based on macro-scale neighborhood composition and micro-scale street characteristics, using street view imagery, POI data, and OSM road network data. The spatiotemporal variations in the influence of built environment factors on street vitality are examined through a multiscale geographically weighted regression (MGWR) model. Results reveal that: (1) Street vitality is most prominent between 10:00 and 20:00, with a spatial pattern of "eastern core, western belt, and multiple clustered points" across all time periods. (2) Macro-scale neighborhood composition generally has a stronger impact on street vitality than micro-scale street characteristics. (3) The influence of various built environment factors on street vitality exhibits significant spatiotemporal heterogeneity. Factors like sky view openness and parking lot density show robust spatiotemporal variations, while connectivity, facility densities, walkability, street ratio, and green view index have localized spatiotemporal effects.

1. Introduction

Streets, as multifunctional aggregators within urban landscapes, not only facilitate the city's daily transportation needs but also serve as vital public spaces for social interaction and leisure activities among residents. Street vitality, perceived through the lens of human activity within these spaces, reflects the concentration of people in streets and stands as a significant indicator of urban vibrancy^[1]. Influenced and constrained by the built environment that accommodates human spatial activities, street vitality is shaped by the continuous organization and succession of urban functions. Both the aggregation of resources at the

macro neighborhood level and the composition of the spatial environment at the micro street level contribute to the temporal and spatial distribution differences of vitality within urban street spaces^[2]. Against the backdrop of high-quality urban development aimed at creating desirable living environments, the quality of urban public spaces has garnered increasing attention from residents. Investigating the impact mechanisms of the built environment on street vitality across multiple scales is crucial for fostering human-centered public spaces and enhancing urban living environments.

* Corresponding author. E-mail address: 2124566697@qq.com

Existing research has predominantly focused on uncovering the effects of the built environment on street vitality, considering both macro neighborhood characteristics and micro street compositions, and has constructed multi-element indicators from perspectives such as location, interface accessibility, functionality, and facilities^[3-5]. Early small-scale case studies based on field research delved into observing interface characteristics, facility arrangements, and landscape compositions within micro street spaces^[4-5]. Subsequently, the advent of the new data wave has expanded the research scale of street vitality through the integration of multi-source big data, with POI and road network data widely applied to measure the density distribution of neighborhood resources and the accessibility of transportation and facilities at the urban scale^[6-7]. However, compared to the detailed measurements at the neighborhood scale that focus on micro street characteristics, the large-scale measurements at the urban scale are limited by data collection and analysis methods, often remaining at the two-dimensional material space level and seldom addressing the micro three-dimensional street space characteristics from the perspective of human subjective perception and experience. Recent advancements in machine learning and image segmentation within the computer science field have provided new methodologies for the large-scale measurement of three-dimensional built environment indicators of streets^[8]. Related studies, based on image semantic segmentation and large-scale image recognition technologies, have automated the extraction of elements such as sky, buildings, and roads from street view images to form three-dimensional built environment indicators of streets, applying these to the measurement and evaluation of street quality^[9-10], urban functional area identification^[11], and urban spatial perception^[12].

In exploring the relationship between the built environment and street vitality, existing research has predominantly employed linear regression models^[13], analyzing the impact differences of various built environment elements on street vitality based on the linear distribution trends of sample values among variables. However, traditional linear regression analysis focuses on exploring the effect of variables on vitality at a global scale through the linear distribution differences of indices, neglecting the spatial distribution patterns of variables at the meso and macro scales. For streets within a city, the similarity of their regional environment and their inherent attractiveness determine a certain degree of similarity and dependency in attracting people among nearby streets^[14], thereby forming a differentiated distribution of vitality and the built environment in space. Recently, scholars have utilized the multi-scale geographically weighted regression model (MGWR) to explore neighborhood vitality^[14], housing prices^[15], the proportion of public transport commuting^[16], and their influencing mechanisms, preliminarily validating its applicability in studying the differentiation of spatial characteristics at the urban scale. This method addresses the lack of consideration for spatial heterogeneity in traditional linear regression models by setting differentiated bandwidths for each variable to form different spatial action scales, thereby provid-

ing a more realistic explanatory power to the overall spatial model^[17-18].

In summary, this paper takes the central urban area of Nanchang as a case study, utilizing POI data and OSM road network data to measure the two-dimensional material space environment, and further employs street view data to measure the micro three-dimensional space environment from the perspective of human subjective perception and experience. Finally, the multi-scale geographically weighted regression model (MGWR) is introduced to explore the temporal and spatial differences in the impact of various built environment elements on street vitality, offering insights and references for the differentiated creation of urban vitality and the enhancement of public space quality.

2. Research Object and Data Sources

2.1. Research Object

The case study area is selected as the central urban area of Nanchang, Jiangxi Province, with its spatial scope defined as the area within the Dongxi Lake District and the Honggutan New District of Nanchang City, which is the concentrated construction area and highly populated area of Nanchang City, covering a total area of approximately 114 km². For convenient comparative analysis, the road network within the research scope is divided into 651 street segments, serving as the basic units for this study (Figure 1). As the traditional core area of the city, the central urban area of Nanchang is the political, economic, and cultural center of Wuhan City, with a large concentration of population, commercial, office, residential, educational, and ad-

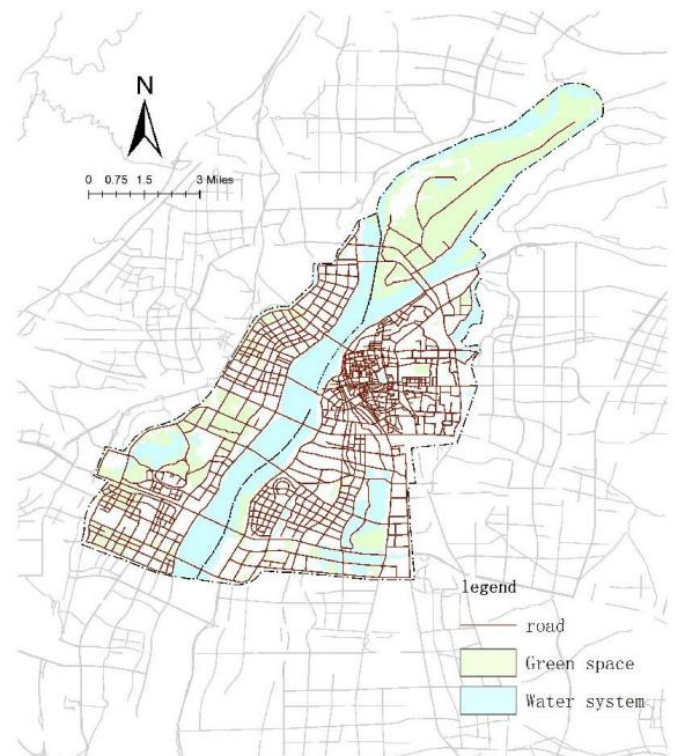


Figure 1 | Distribution of streets in the central urban area of Nanchang

ministrative facilities, forming differentiated urban spatial built environments and human activity distribution characteristics within the region.

2.2. Data Sources and Processing

The basic data of this paper mainly include four categories: road network data, population heat data, street view image data, and POI data:

Road Network Data: The road network data of the central urban area of Nanchang is sourced from the OpenStreetMap website (www.openstreetmap.org). Based on the ArcGIS 10.8 platform, the road network data is cleaned and topologically processed, and then interrupted at intersections. Subsequently, road buffers are constructed based on the road centerline with a buffer distance of 55 meters. This range basically includes the road red line range and its surrounding shops, open spaces, and other areas that may affect street vitality.

Population Heat Data: The population heat data is sourced from the Baidu Map Huiyan Big Data Platform (<https://huiyan.baidu.com>). Using Python to access the server's open port, location service data of the central urban area of Nanchang is collected continuously for 24 hours from May 5, 2025, to May 11, 2025, with the data format being "longitude_latitude_value". Since the activity state of people when using mobile devices is mostly walking or staying, the instantaneous positioning data generated in this state can effectively reflect the real location information of people at specific times^[19].

Street View Data: The street view data is obtained from the Baidu Street View Application Programming Interface (<http://bsyun.baidu.com>). First, based on the vector road network of the central urban area of Nanchang, a sampling point coordinate is obtained every 100 meters, and a Python program is written to call the server interface to obtain panoramic images of the sampling points. A total of 35,687 panoramic street view images are collected starting from May 2024. Then, the PSPNet model pre-trained on the MIT ADE20K dataset is used to semantically segment the panoramic images, identifying and calculating the area proportion of street built environment elements such as sky, green plants, buildings, and roads in the street view images. PSPNet, as a commonly used method in street view image semantic segmentation, effectively reduces the

probability of misidentification by applying a pyramid pooling module to extract and fuse multi-layer features of images, and is one of the current image recognition algorithms with high data classification accuracy^[20].

POI Data: The POI data is sourced from Tencent Maps, with the acquisition time being June 2024. The data covers 16 major categories including food, corporate enterprises, hotels, tourist attractions, and infrastructure, and has advantages in describing the functional diversity of streets and the spatial distribution of stations. Considering the spatial layout forms on both sides of roads of different grades, a total of 132,316 POI points are obtained after intersecting with the street buffers within the research scope through the ArcGIS 10.8 platform.

3. Research Methods and Technical Path

3.1. Indicator Construction

3.1.1. Measurement of Street Vitality Intensity

Referring to existing research on the scale measurement of street vitality, this paper quantifies street vitality as the aggregation intensity of people staying or walking slowly in space. First, based on the acquired location service data, population heat points are visualized on the ArcGIS 10.8 platform according to coordinate information and value values. Second, through kernel density analysis, population heat points are generated into heat grids with a search radius of 200 meters and a cell size of "20 meters x 20 meters", totaling 128 images. Using the natural breakpoint mean of each grid as the division standard, the reclassification tool is used to divide the heat grid values into 7 levels, and then the raster to polygon tool is used to vectorize the graded heat grids. Finally, the vector grids are intersected with each road buffer, and based on the face data with vitality intensity levels within the intersected buffer and the buffer area, a weighted average is performed to obtain the vitality intensity value of each road segment. The specific calculation formula is as follows:

$$Q = \frac{\sum_{i=1}^n A_i Q_i}{\sum_{i=1}^n A_i} \quad (1)$$

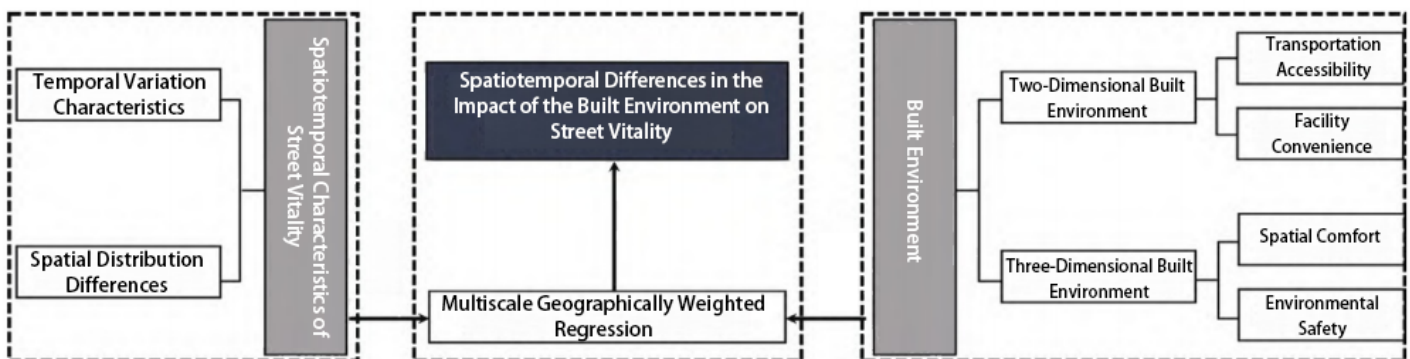


Figure 2 | Technical Path

Table 1 | Calculation statistics of the built environment elements

Built environment	Evaluation level	Evaluation metrics	Quantification of metrics
Two-dimensional built environment	Traffic convenience	The nearest distance to a transportation station	Using the Nearest Facility Point Analysis tool in ArcGIS 10.8 software, the actual distances from the midpoint of streets to the nearest bus stops and subway stations were calculated to reflect the accessibility of the streets
		Parking lot density	The number of parking lots within a 55-meter buffer zone on both sides of the street centerline
		Convenience	The accessibility of a street to nearby streets was analyzed by calculating the ratio of the number of street intersections to the length of the street.
	facility convenience	Functional mixing degree	The location entropy of major points of interest (POIs) within the street buffer zone reflects the diversity of facilities
		Catering function	The ratio of the number of catering facilities within a 55-meter buffer zone on both sides of the street centerline to the length of the street was calculated using the ArcGIS Spatial Join tool
		Entertainment function	The ratio of the number of Entertainment within a 55-meter buffer zone on both sides of the street centerline to the length of the street was calculated using the ArcGIS Spatial Join tool
		Shopping function	The ratio of the number of accommodation hotels within a 55-meter buffer zone on both sides of the street centerline to the length of the street was calculated using the ArcGIS Spatial Join tool
Three-dimensional built environment	Space comfortability	Sky openness	The average proportion of sky elements in street view images within the street unit reflects the degree of spatial openness
		Green light rate	The average proportion of vegetation elements in street view images within the street unit reflects the level of greenery
		Architectural Continuous Process	The standard deviation of the building-to-space ratio within a street reflects the degree of continuity of the building interface.
	environmentl safety	Enclosure degree	The ratio of buildings, walls, columns, fences, and trees within street view images reflects the degree of enclosure in the street space
		Road surface feasibility	The average ratio of pedestrian walkways to roadways within the street reflects the scale of pedestrian space
		Relative pedestrian width	The average ratio of pedestrian pathways to roadways within a street reflects the scale of pedestrian space.
		Traffic safety	The proportion of the midpoint of the street to traffic safety facilities, along with the average ratio of railings and columns within the street, reflects the level of traffic safety, as well as the distance to the nearest subway entrance

Where Q is the street vitality intensity, Q_i is the vitality intensity level corresponding to the i -th unit within the street, A_i is the area of unit i , and n is the number of face data of each level within the road buffer. The built environment indicators that meet the conditions are used as independent variables to construct the MGWR model with street vitality at each time period to explore the temporal and spatial differences in the impact of different built environment elements on street vitality .

3.1.2. Measurement of Built Environment Indicators

Referring to the existing indicator composition of street vitality influencing factors^[21-22], 14 built environment elements are preliminarily selected for measurement from four levels: transportation accessibility, facility conveyed environment includes 8 indicators such as sky openness, enclosure degree, and green view rate, reflectance, spatial comfort, and environmental safety, including two-dimensional spatial environment indicators focusing on macro neighborhood characteristics and three-dimensional spatial environment indicators focusing on micro street composition. Among them, the three-dimensional by the micro street spatial composition environment from the perspective of human subjective perception and experience at the three-dimensional level. These indicators can provide references for the design of local street spaces and the improvement of human settlements. The composition and calculation rules of each indicator are shown in Table 1.

3.2. Analysis Methods

This paper adopts the multi-scale geographically weighted regression model to explain the temporal and spatial differences in the impact of two-dimensional and three-dimensional built environments on street vitality. The multi-scale geographically weighted regression model (MGWR) improves on the classic geographically weighted regression model (GWR) by addressing the limitation that variables can only choose the same bandwidth.

The model sets different bandwidths for each variable to present different scale characteristics. The smaller the bandwidth selected for a variable, the smaller its impact on the overall spatial scale and the stronger its spatial heterogeneity. Conversely, the larger the bandwidth selected for a variable, the more stable it is on the global scale^[23]. The calculation formula is as follows

$$y_i = \sum_{j=1}^k \beta_{bw_j}(u_i, v_i)x_{ij} + \epsilon_i \quad (2)$$

Where X_{ij} is the j -th predictor variable, (U_i, U_v) are the centroid coordinates of street segment i , and β_{bw_j} represents the bandwidth of the regression coefficient for the j -th variable. This study uses MGWR 2.2 software for model calculation and completes visual analysis based on the ArcGIS 10.8 platform

3.3. Technical Path

First, Baidu Huiyan population heat data is used to measure and deconstruct the temporal and spatial variation characteristics of street vitality in the central urban

area of Nanchang at different times of the day. Second, POI data, OSM road network data, and Baidu street view data are used to measure the two-dimensional and three-dimensional built environment. Finally, spatial autocorrelation analysis and linear regression analysis are used to screen variables.

4. Temporal and Spatial Variation Characteristics of Street Vitality in the Study Area

4.1. Temporal Variation Characteristics of Street Vitality Intensity

To intuitively reflect street vitality, the calculated average heat value of streets is represented as a line chart. The statistical results are shown in Figure 3: The fluctuation situation can be roughly divided into four stages: the morning period from 7:00 to 11:00, the noon period from 11:00 to 15:00, the afternoon period from 15:00 to 19:00, and the night period from 19:00 to 23:00. During different times of the day, there are multiple transient heat peaks. Street vitality reaches its first peak at 12:00, consistent with the rapid gathering of people during the morning peak period. From 12:00 to 14:00, it gradually decreases. After that, entertainment and commercial activities in the central urban area gradually become active. Due to the influence of the evening peak and nightlife activities, the number of people in the streets reaches a peak around 20:00, but after that, gathering activities gradually decrease, leading to a rapid decline in street vitality.

The Baidu heat data is divided into 6 levels using the natural breakpoint method, with levels 1-2 classified as low vitality areas, levels 3-4 as medium vitality areas, and levels 5-6 as high vitality areas. The Baidu heat data obtained through vectorization processing is used to count the area proportion of each level, and the proportion of streets with different vitality levels is studied. The statistical results are shown in the table.

Analyzing the proportion of streets with different vitality levels, it can be seen that during the morning peak from 7:00 to 9:00, the proportion of high vitality streets and medium vitality streets is low, and they start to rise with

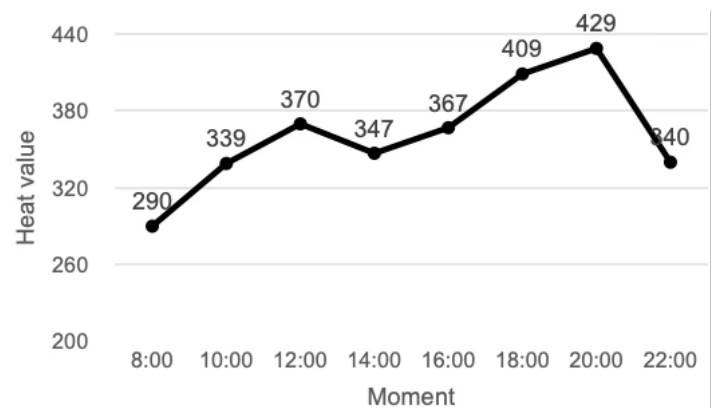


Figure. 3 | Variation of Overall Street Vitality in the Central Urban Area of Nanchang

Table 2 | Statistics of Instantaneous Vitality Intensity Proportion in Streets of Central Urban Area of Nanchang

Time period	Type of fluctuation	Heat value	Volatility
07:00-11:00	Rapid rise	290-339	0.17
11:00-13:00	Slowly rising	339-370	0.09
13:00-15:00	Slow descent	370-347	-0.06
15:00-17:00	Slowly rising	347-367	0.06
17:00-19:00	Rapid rise	367-409	0.11
19:00-21:00	Slowly rising	409-429	0.05
21:00-23:00	Fast descent	429-340	-0.21

roughly the same trend. Due to the relatively dispersed distribution of people during lunch time, the proportion of high vitality streets and medium vitality streets shows a slow downward trend from 11:00 to 13:00. At 18:00 in the afternoon, the proportion of medium vitality streets is relatively high, reaching a vitality peak. At 20:00 at night, the proportion of high vitality streets is relatively high, reaching a vitality peak, while the proportion of medium vitality streets is relatively low. This phenomenon can be attributed to the further gathering of people's activities in the central urban area at night. It can be inferred that the intensity of people's activities in the morning is usually higher than that during the noon period. The density of people in the neighborhood gradually increases after lunch time, indicating that the leisure activities of neighborhood people usually reach a peak from after lunch time to the evening.

4.2. Spatial Differentiation Characteristics of Street Vitality Intensity

To further explore the spatial differentiation characteristics of street vitality at different times of the day, especially during the main activity periods, the average vitality of streets during four time periods: 7:00-11:00 (morning), 11:00-15:00 (noon), 15:00-19:00 (afternoon), and 19:00-23:00 (night) is visualized. The analysis results in the spatial distribution map of the comprehensive heat value of streets on weekdays (Figure 4). From Figure 4, it can be seen that the overall street vitality in the central urban area of Nanchang shows a spatial differentiation pattern of "east core, west belt, multi-point aggregation", with medium and high value areas forming differentiated distributions with time changes. It can be seen that high vitality streets and medium vitality streets on weekdays are mostly concentrated in the central part of the old city, and the vitality of streets in the north is significantly higher than that in the south. Specifically, high vitality streets are mainly con-

Table 3 | Statistics of Instantaneous Vitality Intensity Proportion in Streets of Central Urban Area of Nanchang

	8:00		10:00		12:00		14:00	
	Quantity	Ratio	Quantity	Ratio	Quantity	Ratio	Quantity	Ratio
High-energy street	10	1.54%	30	4.61%	45	6.91%	33	5.07%
Mid-energy street	96	14.75%	123	18.89%	118	18.13%	112	17.20%
Low-energy street	545	83.72%	498	76.50%	488	74.96%	506	77.73%
	16:00		18:00		20:00		22:00	
	Quantity	Ratio	Quantity	Ratio	Quantity	Ratio	Quantity	Ratio
High-energy street	44	6.76%	55	8.45%	71	10.91%	48	7.37%
Mid-energy street	136	20.89%	147	22.58%	102	15.67%	95	14.59%
Low-energy street	471	72.35%	449	68.97%	478	73.43%	508	78.03%

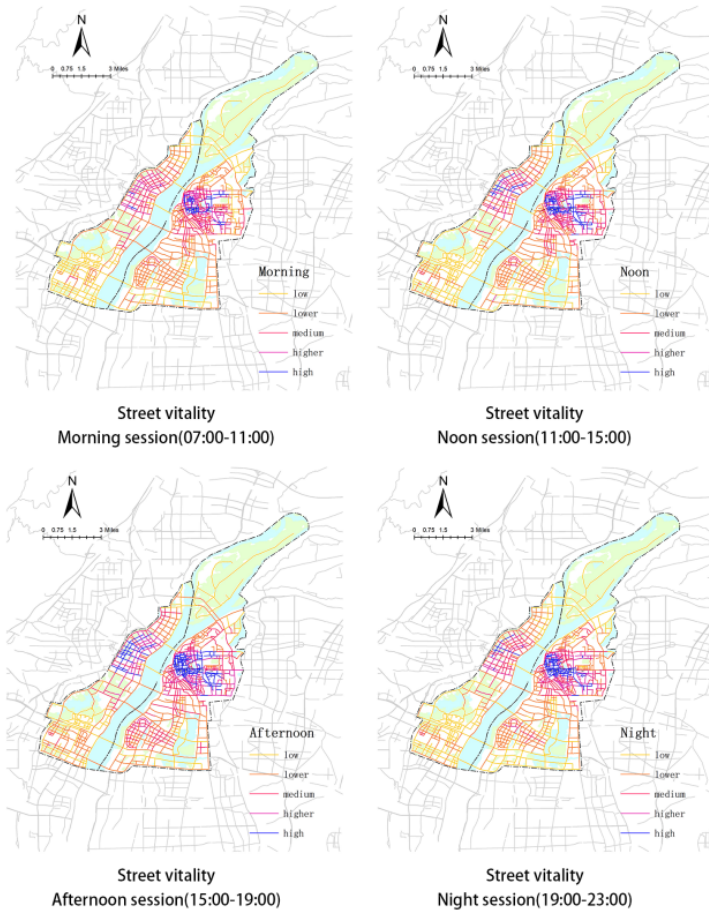


Figure 4 | Spatial Variation of Street Vitality Intensity Across Different Time Periods

centrated in the cultural and tourism integration area within the Wanshou Palace historical urban area and the traditional commercial center area of Zhongshan Road-Shengli Road Pedestrian Street. Although this area is an old city, it has a large concentration of shopping, dining, and accommodation resources, rich tourism resources, complete public service functions, and well-equipped living facilities. Secondly, the central area of Honggutun, centered on Central Financial Street, also has high street vitality, including CBD, Qiushui Square, etc. This area has well-equipped commercial facilities and high transportation accessibility, making it easy to gather vitality. It can be seen that the street vitality in the central urban area shows a trend of decreasing from the central area on both sides of the Gan River to the suburbs, and a distribution of central aggregation and stronger north than south.

5. Spatiotemporal Heterogeneity in the Impact of Street-Level Built Environment on Urban Vitality Intensity: a Multiscale Analysis

5.1. Analytical Framework for MGWR Model Results

5.1.1. Screening of Built Environment Indicators

First, spatial autocorrelation analysis is conducted on the 14 built environment indicators, and the results show that all variables have obvious clustering characteristics in space. From the global Moran's index statistics, the nearest distance to comprehensive shopping malls, proximity, and the nearest distance to transportation stations have very strong clustering characteristics (Table 4). Then, ordinary least squares (OLS) is further used to perform regression analysis with the 14 multi-dimensional built envi-

Table 4a | Results of Spatial Autocorrelation and Multicollinearity Diagnostics for the Built Environment

First-level indicators	Two-dimensional built environment						
	Traffic convenience				facility convenience		
Secondary indicators	Transportation distance	Parking lot density	Connectivity	Functional mixing degree	Catering function	Entertainment function	Shopping function
Global Moran's index Numeric	0.440341	0.334867	0.682102	0.252610	0.167312	0.297193	0.777576
Space-time self-correlation							
Variance	0.000004	0.000004	0.000004	0.000004	0.000004	0.000004	0.000004
Z score	171.765156	225.414225	348.521286	129.080649	85.559826	152.102850	397.443716
P-value	0.000000	0.000000	0.000000	0.000000	0.000000	0.000000	0.000000
Collinearity Diagnosis							
Variance inflation factor	1.563141	1.494003	1.590602	1.645913	1.385783	1.747346	1.505872

Table 4b | Results of Spatial Autocorrelation and Multicollinearity Diagnostics for the Built Environment

First-level indicators		Three-dimensional built environment						
		Space comfortability				environmentl safety		
Secondary indicators		Sky openness	Green light rate	Architectura Continuous Process	Enclosure degree	Road surface feasibility	Relative pedestrian width	Traffic safety
Space-time self-correlation	Global Moran's index Numeric	0.144728	0.235639	0.089482	0.317182	0.084996	0.089482	0.112461
	Variance	0.000004	0.000004	0.000004	0.000004	0.000004	0.000004	0.000004
	Z score	171.765156	162.072935	45.788505	129.080649	45.194476	185.559826	57.571604
	P-value	0.000000	0.000000	0.000000	0.000000	0.000000	0.000000	0.000000
Collinearity Diagnosis	Variance inflation factor	1.252827	1.371032	1.420298	3.133947	1.065539	1.385783	1.058528

ronment elements as independent variables and the street vitality values at each time period as dependent variables. The results show that the VIF values of all independent variables are far below 75 (Table 4), indicating that there is no multicollinearity problem among the variables. However, the probability p-values of relative pedestrian width and building continuity are greater than 0.01 in all time periods, indicating that their impact on street vitality is not significant and needs to be excluded. Finally, the remaining 12 built environment indicators participate in the subsequent model construction.

5.1.2. Model Regression Results

According to the temporal variation characteristics of street vitality intensity, the street vitality and built environment indicators of the four time periods are introduced into the multi-scale weighted regression model for analysis (Table 5). The results show that the average adjusted R² of the MGWR model in each time period is 0.844, indicating that its overall explanation degree of street vitality changes in the central urban area of Nanchang is as high as 84.4% on average. Subsequently, based on the regression coefficients, variable interpretability, and spatial action scale (bandwidth), the temporal and spatial effects of different built environment elements on street vitality in each time period are further analyzed. The regression coefficients of the three-dimensional built environment indicators are relatively high overall, but there are differences in variable influence and interpretability in different time periods.

5.2. Spatiotemporal Differences in the Impact of Two-Dimensional Built Environment on Street Vitality

5.2.1. Temporal Differences in the Two-Dimensional Built Environment

(1) Transportation Accessibility

Parking lot density showed a positive correlation with street vitality across all time periods, with higher significance overall. Its influence was stronger in the morning and midday compared to the afternoon and evening, indicating that the capacity for vehicle parking in street spaces positively promotes vitality. Connectivity also demonstrated a positive impact on vitality, particularly during daytime hours when pedestrian accessibility attracts natural travel choices. However, the average distance to the nearest transportation hub exhibited a negative correlation with street vitality across all periods, though its explanatory power was negligible. This may be due to the relatively balanced distribution of transportation hubs in Nanchang's central urban area^[25], resulting in minimal differences in accessibility between streets (Figure 5).

Facility Accessibility

The explanatory power of dining facilities on street vitality (37.79%-68.97%) remained consistently high across all periods. This is primarily because dining facilities cater to various needs throughout the day, including breakfast, lunch, afternoon tea, dinner, and late-night snacks, ensuring a steady flow of people and sustaining street vitality. Shopping facilities had the highest absolute regression coefficients (0.159-0.234) across all periods, with their positive influence peaking during the evening. Their explanatory power (51.31%-70.20%) was also consistently high, highlighting the strong promotional effect of commercial activities on street vitality. However, the localized clustering

Table 5 | Statistical Summary of Regression Results from the Multiscale Geographically Weighted Regression (MGWR) Model

Variable	07:00-11:00			11:00-15:00			15:00-19:00			19:00-23:00		
	Bandwidth	Average value	Variable interpretability									
The nearest distance to a transportation station	221	-0.053	0	189	-0.012	0	650	-0.041	0	650	-0.023	0
Parking lot density	646	0.082	100	650	0.081	100	507	0.075	73.58	650	0.057	57.93
Convenience	650	0.181	80.65	650	0.133	57.31	252	0.136	57.30	268	0.118	56.99
Functional mixing degree	650	-0.065	0	650	-0.066	0	650	-0.067	0	650	-0.115	0
Catering function	650	0.070	37.79	650	0.072	58.06	650	0.093	58.06	650	0.074	68.97
Entertainment function	650	0.002	14.75	650	0.010	17.97	650	0.011	51.77	650	0.009	39.63
Shopping function	257	0.159	62.83	236	0.158	70.20	249	0.195	51.31	236	0.234	70.20
Sky openness	650	-0.348	100.00	650	-0.073	100.00	650	-0.327	77.57	650	-0.338	100
Green light rate	338	0.605	0	198	-0.227	0	439	0.571	0	447	0.787	0
Enclosure degree	431	-1.313	0	650	0.108	0	431	-1.244	0	419	-1.568	0
Road surface feasibility	295	0.011	74.50	650	0.001	64.71	650	0.003	59.91	650	0.011	35.94
Traffic safety	650	0.216	53.92	650	0.032	54.84	650	0.205	36.71	148	0.257	14.13
Adjusted R-squared		0.835			0.843			0.852			0.846	

Note: Variable interpretability represents the percentage of the total sample size with significant coefficients ($p \leq 0.05$) for explanatory variables.

of commercial facilities led to spatially significant variations in their explanatory power.

Entertainment facilities showed an increasing positive correlation with street vitality as the day progressed, peaking in the evening. This indicates that the impact of leisure and entertainment facilities on street vitality is more pronounced at night due to their primary usage times. Functional mix exhibited a negative correlation with street vitality across all periods, suggesting that streets with lower functional mix tend to concentrate vitality more effectively. Specifically, streets dominated by single-use commercial activities are more likely to attract consumer behavior, with clear travel purposes for various facilities, especially at night.

5.2.2. Spatial Differences in the Two-Dimensional Built Environment

To explain the spatial heterogeneity of the influencing factors, ArcGIS 10.8 was used to visualize the coefficients of significant factors during the main activity periods. The spatial patterns of some variables are shown in Figures 6 and 7. Overall, connectivity, as a global variable, exhibited the most stable spatial influence on street vitality, followed by parking lot density. Entertainment and dining facilities showed significant spatial heterogeneity, while shopping facilities displayed distinct spatial differentiation.

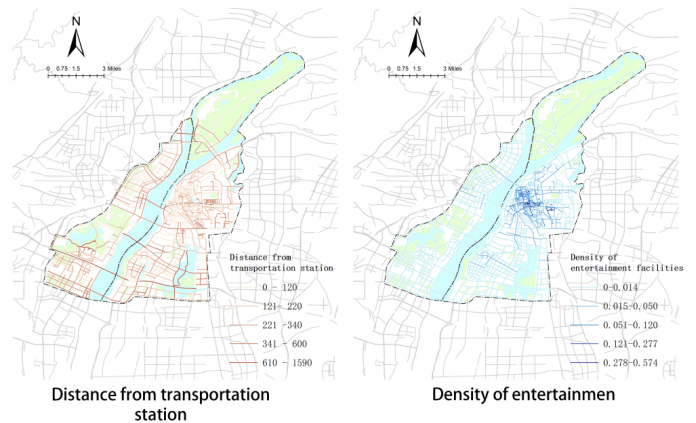


Figure 5 | Distribution of the Nearest Distance to Transportation Stations and Density of Entertainment Facilities in Streets

Specifically, the impact of connectivity on street vitality showed minimal spatial variation, with its positive influence gradually increasing from north to south throughout the day. High-value areas were concentrated in Jiuzhou and Chaonong streets in Xihu District, where parks and educational facilities are abundant, facilitating pedestrian activity.

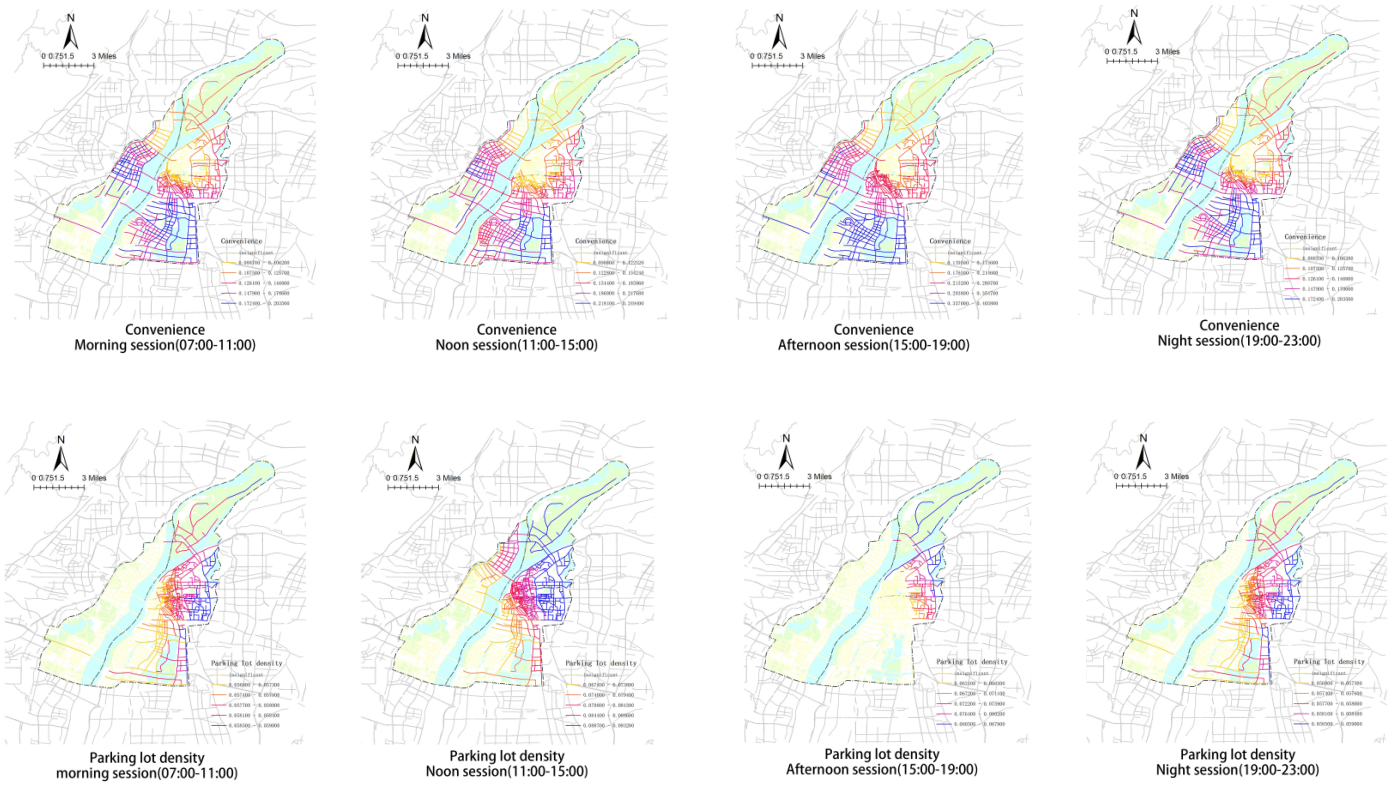


Figure 6 | Spatial Distribution of Regression Coefficients for Traffic convenience

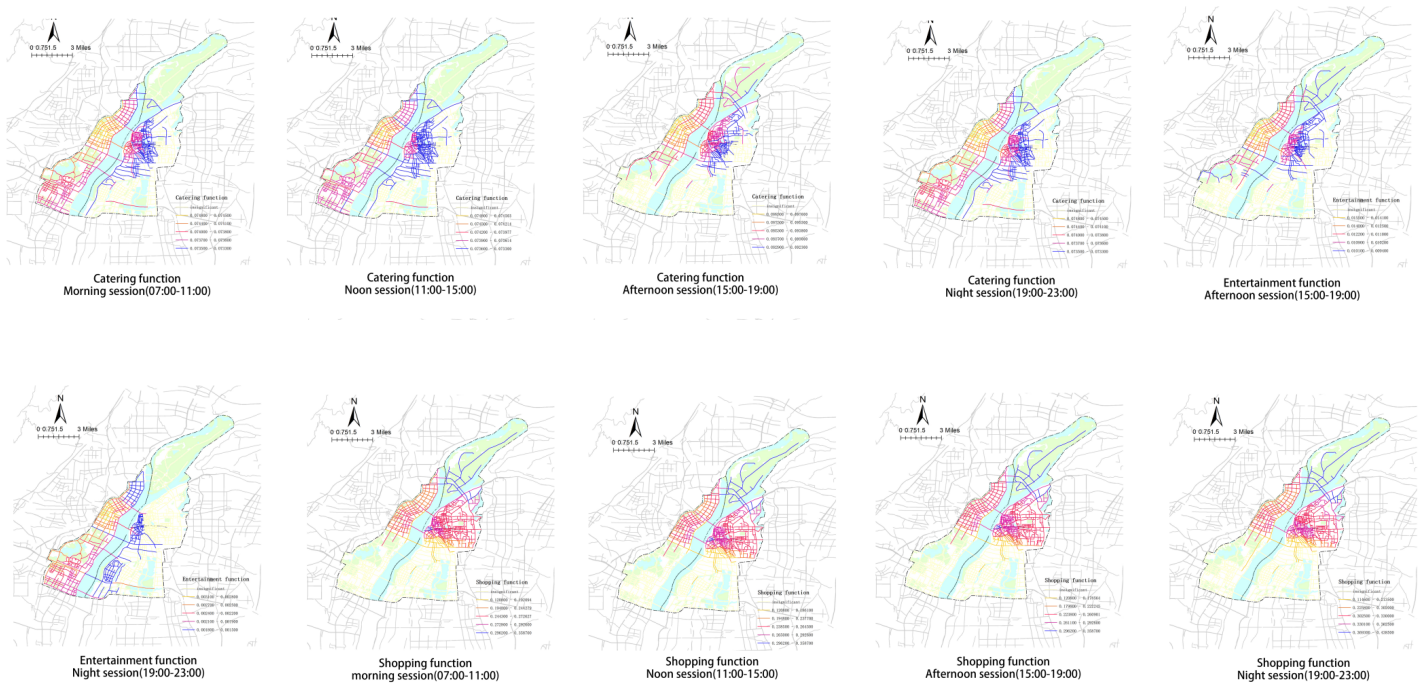


Figure 7 | Spatial Distribution of Regression Coefficients for Facility Convenience

ties such as sightseeing and commuting. In contrast, areas like Honggutan District's Hongjiaozhou and Jiulonghu streets, as well as Baihuazhou Street in the historical district, showed no significant impact due to the high density of transportation and educational facilities, which attract

purpose-driven pedestrians unaffected by street connectivity.

The positive impact of parking lot density on street vitality generally increased from the central to the western areas. High-value areas were clustered in Dinggong Road and Pengjiaqiao streets in Donghu District, where limited

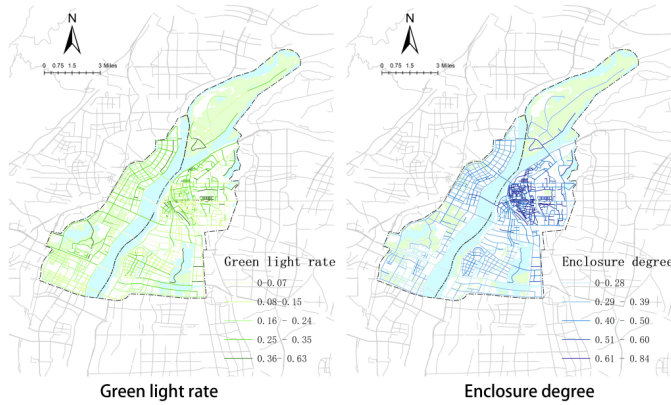


Figure 8 | Distribution of Green View Index and Enclosure Rate



Figure 9 | Spatial Distribution of Regression Coefficients for Spatial Comfort

vehicle access in the historical district necessitates parking before entering, enhancing the influence of parking density on vitality. In other areas, the availability of public transportation, such as subways and buses, reduced the reliance on parking facilities.

Dining facilities exhibited a positive influence on street vitality that decreased from the central to the western areas. High-value areas were concentrated in Dinggong Road and Shengjin Tower streets in Donghu District, where local cuisine in the old town enhances street attractiveness. Entertainment facilities showed positive correlations and significance in the afternoon and evening, with their influence decreasing from the central to the western areas. High-value areas were mainly located in the historical dis-

tricts of Donghu and Xihu Districts, where abundant tourism and leisure resources attract visitors and sustain high street vitality.

Commercial facilities displayed localized clustering in their positive influence on street vitality, with high-value areas concentrated in Tengwang Pavilion Street in Xihu District and Shajing Street in Honggutuan District. These areas feature a mix of traditional and chain commercial establishments, attracting both local residents and tourists and enhancing street vitality.

5.3. Spatiotemporal Differences in the Impact of Three-Dimensional Built Environment on Street Vitality

5.3.1. Temporal Differences in the Three-Dimensional Built Environment

As shown in Figure 8, the regression coefficients of the built environment indicators across the four time periods were generally low, with significant variations in influence and explanatory power across different periods.

Spatial Comfort

The explanatory power of green view ratio and enclosure degree was negligible. This may be due to the dispersed distribution of greenery along roads and the relative clustering of vegetation around natural landscapes, rendering the green view ratio ineffective in explaining vitality. High pedestrian flow streets may not be significantly affected by enclosure degree, as the existing foot traffic is sufficient to sustain street vitality. Sky view openness exhibited a negative correlation and was significant across all four periods. Its negative influence gradually increased during the daytime, peaking in the afternoon. This is likely because streets with high sky view openness often lack building or tree cover, leading to functional monotony and a lack of commercial, cultural, or social activities that attract pedestrians. In the afternoon, people tend to gather in work areas, amplifying the impact of sky view openness on street vitality.

Environmental Safety

The average regression coefficient of walkability ratio showed a positive correlation with street vitality across all periods, with high explanatory power (35.94%-74.50%). Its positive influence was stronger in the morning and afternoon, as these periods involve commuting activities. A well-maintained pedestrian environment supports walking, cycling, and other modes of transportation, increasing street usage and attracting more customers, thereby promoting commercial activity. In contrast, traffic safety facilities had lower explanatory power (14.13%-54.84%), with their positive influence peaking in the afternoon when commuting demand is high. Properly designed traffic facilities can optimize traffic flow, reduce congestion, and enhance street attractiveness.

5.3.2. Spatial Differences in the Three-Dimensional Built Environment

As shown in Figure 9, sky view openness, as a global negative correlation variable, exhibited a spatial pattern of higher influence in peripheral areas and lower influence in central areas. High negative impact areas were concen-

midday and afternoon periods. This is because these periods involve diverse pedestrian activities, and the historical district's commercial vibrancy, combined with fewer vehicle lanes, enhances the pedestrian environment, attracting more customers and promoting commercial activities.

6. Conclusions and Discussion

This paper takes the central urban area of Nanchang as a case study, uses population heat data to measure and deconstruct the temporal and spatial differences of street vitality, uses OSM road network data and POI data to measure the two-dimensional material space environment, further uses street view images to measure the micro three-dimensional street space environment based on human subjective perception and experience, and uses the multi-scale geographically weighted regression model to explore the differentiation characteristics of multi-dimensional built environment and urban street vitality in time and space. The main conclusions are as follows.

The temporal and spatial distribution differences of street vitality in the central urban area of Nanchang are obvious. In terms of time, residents' activities on the streets are mostly concentrated from 6:00 to 23:00, with the highest proportion of medium and high vitality streets from 9:00 to 18:00. In terms of space, the spatial structure of street vitality generally shows a differentiation pattern of "east core, west belt, multi-point aggregation", and the aggregation characteristics are most obvious in the afternoon.

The impact of the two-dimensional built environment on street vitality is generally more significant than that of the three-dimensional built environment. Specifically, among the two-dimensional built environment indicators, parking lot density, connectivity, and shopping facility density have high interpretability for street vitality in all time periods, while catering facility density and entertainment function have high interpretability in some time periods. Among the three-dimensional built environment indicators, only sky openness and road surface feasibility have high interpretability for street vitality in most time periods.

The temporal and spatial heterogeneity of the impact of each built environment element on street vitality is obvious. In terms of transportation accessibility, the positive influence of connectivity on street vitality generally increases from north to south in space in all time periods

Data availability: Data will be made available on request.

Competing Interests: The authors declare that they have no known competing financial interests or personal relationships that could have appeared to influence the work reported in this paper.

1. Long Y ,Zhou Y, Study of chengduQuantitative Evaluation on Street Vibrancy and its impact Factors: A Case [J]. New Construction ,2016(1):52- 57.
2. Wu W J, Wu L Y, Shi X D, et al. Human Settlements and High-quality Development [J]. Urban Planning,2020,44(1):99-104.
3. Wang B L, Spatial impact of the built environment on street vitality: a case study of the Tianhe district, Guangzhou[J]. Frontiers in environmental science, 2022, 10: 966562.
4. Jiang L, Quantitative Assessment and Shaping Strategies for Urban

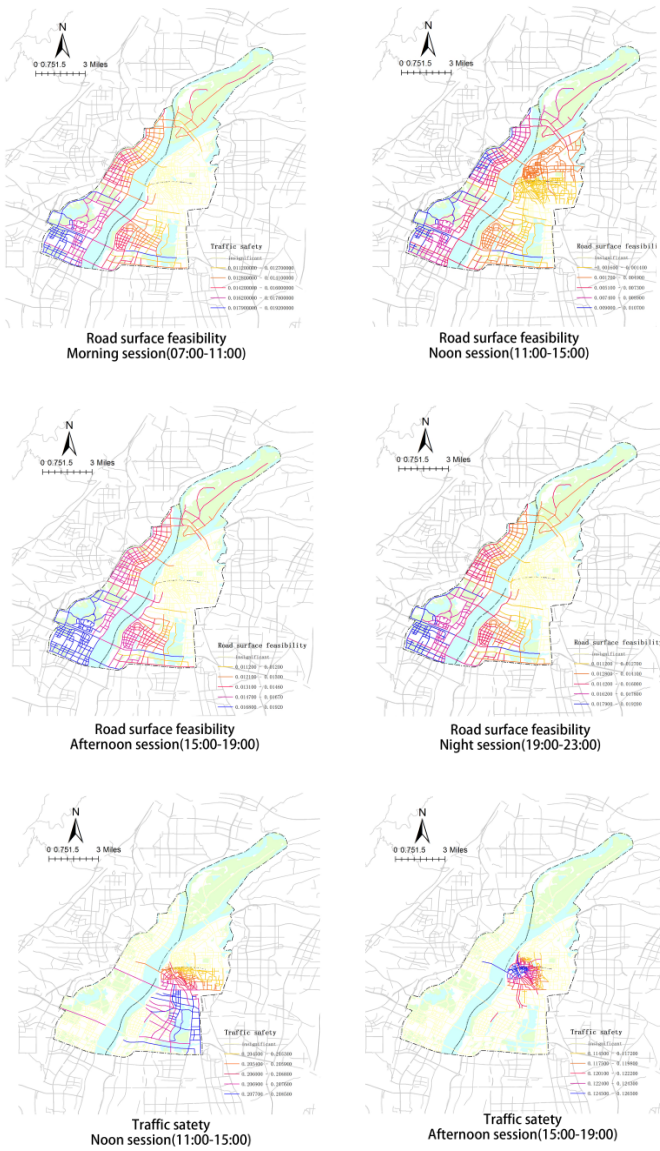


Figure 10 | Spatial Distribution of Regression Coefficients for Traffic Safety

trated in Hongjiaozhou and Jiulonghu streets in the south-western part of the central urban area, where large transportation and entertainment facilities dominate, and pedestrian activities are more purpose-driven. In contrast, Tao-hua Street and Shengjin Tower Street in the southern historical district showed relatively lower impacts on street vitality. These areas feature scenic landscapes and iconic buildings, where high sky view openness does not significantly affect pedestrian destinations or street activities.

As shown in Figure 10, the positive influence of walkability ratio on street vitality exhibited a spatial pattern of higher values in the west and lower values in the east. High-value areas were concentrated in Hongjiaozhou and Jiulonghu streets in the Honggutan New District, with additional clustering in Shajing Street during midday. This may be due to the presence of large commercial and office facilities in these areas, where pedestrians primarily use sidewalks for dining and commuting activities during lunchtime. The influence of traffic safety facilities on street vitality was concentrated near the historical district during

- Street Vitality [D]. Dalian : Dalian University of Technology ,2013.
5. Huang D, DAI D H, Effect of Living Street's Elements on Vitality—Taking Typical Streets in Shenzhen as an Example [J]. *Chinese Landscape Architecture* ,2019,35(9):89-94.
 6. Huang S H, WANG C S, Street Urbanism : Street Urbanism:Quantitative Evaluation on Wuhan Street Vibrancy and Its Impact Factors [J]. *Shanghai Urban Planning Review* ,2020(1):105-113.
 7. Wang P, Long Y, Shi M, et al. Street Vibrancy of Beijing: Measurement, Impact Factors and Design Implication [J]. *Shanghai Urban Planning Review* ,2016(3):37-45.
 8. Long Ying , Tang J X, Large-Scale Quantitative Measurement of the Quality of Urban Street Space: The Research Progress [J]. *City Planning Review* ,2019,43(6):107-114.
 9. Guo X, Lai J D, Ma Z f, et al. Consistency analysis between virtual evaluation and on-site survey methods for street quality: A case study of streets in Shenzhen's core transit areas. [J]. *Planners* ,2022,38(6):70-78.
 10. Chen C, Chen Q J, Jia Z M, et al . Large-scale Measurement of the Quality of Urban Street Space Based on Physical Disorder Theory: A Case Study of Area within the Second Ring of Hefei City [J]. *Southern Architecture* ,2020(2):10- 18.
 11. Wan J Q, Fei T. "ProductionLiving-Ecological Spaces" recognition method based on street view images[J]. *Journal of Geo-information Science*, 2023,25(4):838- 851.
 12. Wu C, Ye Y, Gao F, et al. Using street view images to examine the association between human perceptions of locale and urban vitality in Shenzhen, China[J]. *Sustainable cities and society*, 2023, 88: 104291.
 13. Niu X Y, Wu W S, Li M. LBS Positioning Data Influence of Built Environment on Street Vitality and Its Spatiotemporal Characteristics Based on [J]. *Urban Planning International* ,2019,34(1):28-37.
 14. Fan L: Zhang D Y . Research on the Influence Mechanism and Spatial Heterogeneity Characteristics of Block Vitality in Beijing: Based on Multi-Scale Geographically Weighted Regression[J]. *City Planning Review* ,2022,46(5):27-37.
 15. Shen T, Yu H C, Zhou L, et al. On Hedonic Price of Second-Hand Houses in Beijing Based on Multi-Scale Geographically Weighted Regression:Scale Law of Spatial Heterogeneity [J]. *Economic Geography* ,2020,40(3):75-83.
 16. An R, Wu Z, Tong Z, et al. How the built environment promotes public transportation in Wuhan: a multiscale geographically weighted regression analysis[J]. *Travel behaviour and society*, 2022, 29: 186-199.
 17. Lao X, Gu H, Unveiling various spatial patterns of determinants of hukou transfer intentions in China: a multi-scale geographically weighted regression approach[J]. *Growth and change*, 2020, 51(4): 1860-1876.
 18. Wu C, Ren F, Hu W, et al. Multiscale geographically and temporally weighted regression: exploring the spatiotemporal determinants of housing prices[J]. *International journalofgeographicalinformation-science*,2019,33(3):489-511.
 19. WU Z Q, YE Z N, Research on Urban Spatial Structure Based on Baidu Heat Map: A Case Study on the Central City of Shanghai[J].*City Planning Review*,2016,40(4):33-40.
 20. ZHAO H, SHI J, QI X, et al. Pyramid scene parsing network[C]//Proceeding of IEEE Conference on Computer Vision and Pattern Recognition. New York: IEEE, 2017.
 21. Si R, Lin Y Y, Xiao Z P, et al. Spatio-temporal analysis of built environment and street vitality relationship based on street-level imagery: A case study of Futian District, Shenzhen. *Scientia Geographica Sinica*,2021,41(9):1536-1545.
 22. MAO Z R, CHEN X K, XIANG Z H, et al. Research on the Measurement and Influencing Factors of Street Vigour in Historic Districts: A Case Study of Wenming Street Historic District in Kunming[J]. *South Architecture*, 2021 (4):48-55.
 23. FOTHERINGHAM, YANGW, KANGW. Multiscale geographically-weighted regression (MGWR)[J]. *Annals of the American Association of Geographers*, 2017, 107(6):1247-1265.
 24. WANG Lucang. Central Areas of Wuhan City Spatial-temporal Characteristics of Urban Population Aggregation Based on Baidu Heat Map in[J]. *J. Sustain. Habitat West. China*, 2018, 33(2):52-56.
 25. Ren P, Peng J D, Yang H, et al. Relationship between jobs-housing balance and built environment in areas around urban rail transit stations of Wuhan[J]. *Journal of Geo-information Science*, 2021, 23(7):1231-1245.